JOURNAL OF AIRCRAFT
Vol. 31, No. 1, Jan.–Feb. 1994

Unsteady Vortex Structure over a Delta Wing

Raymond E. Gordnier* and Miguel R. Visbal*
U.S. Air Force Wright Laboratory, Wright-Patterson Air Force Base, Ohio 45433

The structure of the shear layer which emanates from the leading edge of a 76-deg sweep delta wing and forms the primary vortex is investigated numerically. The flow conditions are $M_\infty = 0.2$, $Re = 50{,}000$ and angle of attack of 20.5 deg. Computational results are obtained using a Beam-Warming-type algorithm. The existence of a Kelvin-Helmholtz-type instability of the shear layer which emanates from the leading edge of the delta wing is demonstrated. A description is provided of the three-dimensional, unsteady behavior of the small-scale vortices associated with this instability. The numerical results are compared qualitatively with experimental flow visualizations exhibiting a similar behavior.

Introduction

THE present work has developed out of a series of experimental and computational investigations of the following background. Gad-el-Hak and Blackwelder[1] observed for water tunnel tests of two delta wings that the vortex sheet which emanates from the leading edge of the delta wing rolls up into discrete vortices that undergo a pairing process. The instability appears as alternating dark and light regions in the dye sheet near the leading edge of the delta wing and extending along it (Fig. 1). This instability is said to be similar to the instability and vortex pairing process described by Brown and Roshko[2] and Winant and Browand[3] for two-dimensional shear layers. Both are related to the classical Kelvin-Helmholtz-type instability of two-dimensional shear layers and are distinct from the von Karman-type shedding observed by Rediniotis et al.[4] for high angles of attack.

In another water tunnel investigation of the leading-edge vortices on delta wings, Shi et al.[5] also observe small-scale vortices that are periodically shed from the leading edge of the delta wing. This phenomena is related to that observed by Gad-el-Hak.[1] Contrary to the observations of Gad-el-Hak, Shi et al.[5] observe no vortex pairing of these small-scale vortices.

Payne et al.[6] also observed an instability in the shear layer forming the primary vortex using smoke flow visualization techniques. They again relate the growth of these secondary structures to the classical Kelvin-Helmholtz type of instability. The authors report that the vortical structures are static, however, and do not rotate with the vortex. They also relate these observations[7] to those of Gad-el-Hak and Blackwelder.[1]

Lowson[8] has carried out low-speed wind-tunnel tests to investigate the vortex sheet structure formed about delta wings. In this work he concludes that not one, but two distinct types of instability exist. The first, shown in Fig. 2, is the quasi-two-dimensional type of instability of the shear layer leaving the leading edge observed by Gad-el-Hak.[1] The second is a locally streamwise instability of the feeding vortex sheet that gives rise to steady vortex cell structures within the vortex core. Lowson suggests that this is the instability observed by Payne et al.[6]

All these experimental results have been obtained for scaled models at relatively low Reynolds number. Recent photographic evidence shows that similar types of secondary vortical structures are observed for the LEX vortex flow on an F-18 in flight.[9] This strongly indicates that the vortex structure found experimentally at lower Reynolds number occurs in flight conditions at full-scale Reynolds number.

A similar type of shear-layer instability is observed by the present authors[10] in calculations for a 76-deg sweep delta wing at 20.5-deg angle of attack and a Reynolds number of 900,000. An unsteady behavior of the shear layer which emanates from the leading edge of the delta wing, related to the instability described by Gad-el-Hak and Blackwelder,[1] is found in these calculations. In the current work, further computations are performed at a lower Reynolds number, $Re = 50{,}000$, and for enhanced grid resolution. An improved description of the observed unsteady process will be given. The lower values of Reynolds number provide the ability to relate the numerical results to the existing experimental observations just described.

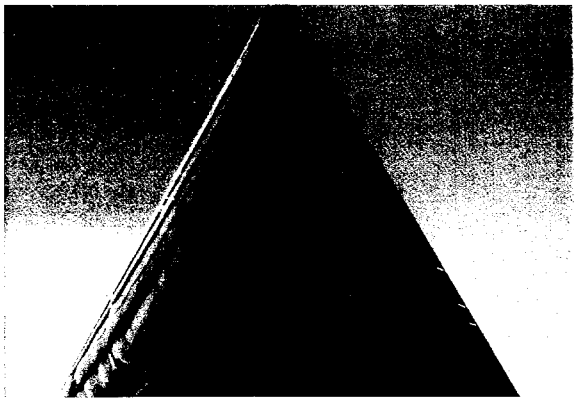

Fig. 1 Dye sheet visualization showing small-scale vortices for a 60-deg sweep delta wing, $\alpha = 10$ deg.[1]

Fig. 2 Smoke flow visualization of vortex over a 70-deg sweep delta wing at 20-deg angle of attack.[8]

Received April 30, 1992; revision received Oct. 6, 1992; accepted for publication Oct. 16, 1992.

*Aerospace Engineering. Member AIAA.

Governing Equations

The governing equations for the present problem are the unsteady, three-dimensional, full Navier-Stokes equations written in strong conservation form[11] using a general coordinate transformation ξ, η, ζ, t

$$\frac{\partial}{\partial t}\left(\frac{q}{J}\right) + \frac{\partial \hat{F}}{\partial \xi} + \frac{\partial \hat{G}}{\partial \eta} + \frac{\partial \hat{H}}{\partial \zeta} = \frac{1}{Re}\left[\frac{\partial \hat{F}_v}{\partial \xi} + \frac{\partial \hat{G}_v}{\partial \eta} + \frac{\partial \hat{H}_v}{\partial \zeta}\right] \tag{1}$$

where

$$q = [\rho \quad \rho u \quad \rho v \quad \rho w \quad \rho E_t]^T$$

Here $\hat{F}$, $\hat{G}$, and $\hat{H}$ are the inviscid fluxes and $\hat{F}_v$, $\hat{G}_v$, and $\hat{H}_v$ are the viscous fluxes in the ξ, η, and ζ directions, respectively. The system of equations is closed using the perfect gas law, Sutherland's formula for viscosity, and the assumption of a constant Prandtl number, $Pr = 0.72$. Flow quantities have been nondimensionalized by their respective freestream values except for pressure, which is nondimensionalized by twice the freestream dynamic pressure, and speed of sound which is nondimensionalized by the freestream velocity. All lengths have been normalized by the root chord length of the delta wing.

Numerical Procedure

The governing equations are solved numerically using the implicit approximately factored algorithm of Beam-Warming.[12] The equations are differenced using Euler implicit time-differencing and second-order accurate central differences for all spatial derivatives. A blend of second- and fourth-order nonlinear dissipation, as suggested by Jameson,[13] is used to stabilize the central difference scheme. The current work, in which subsonic flows are investigated, requires only fourth-order dissipation. A subiteration procedure[14] is also included to improve the stability characteristics of the scheme when necessary by reducing factorization errors in the three-factored scheme.

A fully vectorized, time-accurate solver has been developed to implement the aforementioned scheme.[15] The computational requirements of the scheme are approximately 38 words/grid point and 4.4×10^{-5} CPU s/grid point/iteration on a Cray 2. This code has been validated for a number of unsteady laminar flows.[15-18] These results provide a good validation base for the code. Most importantly, the results of Ref. 15 demonstrate the ability to correctly simulate naturally occurring instabilities in the flowfield and the transition of the flow from steady to unsteady behavior.

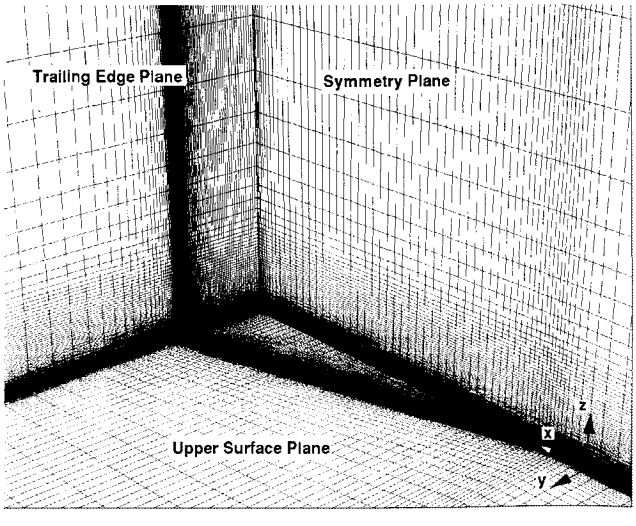

Fig. 3 Delta wing grid.

The computational grid (Fig. 3) for the delta wing was obtained using simple algebraic grid generation techniques. The grid structure is of H-H type with planar grids being stacked in the axial direction. The H-H structure provides for good resolution of the sharp leading edge with no rounding. All far-field boundaries are located 1.5–2 chord lengths away from the delta wing.

The boundary conditions are implemented in the following manner. On the wing surface, the no-slip condition for the velocities, adiabatic wall temperature condition, and zero normal pressure gradient condition are used. At the downstream boundary, flow variables are extrapolated from the interior. Symmetry conditions are imposed along the midplane of the wing. Characteristic boundary conditions[19] are used at the upper, lower, side, and upstream boundaries.

Results

High Reynolds Number Case

All results presented are calculated for a 76-deg sweep, aspect ratio 1 delta wing. This configuration has been investigated experimentally by Hummel.[20] The first calculations for this configuration[10] are made at Reynolds number 900,000, angle-of-attack of 20.5 deg, and a freestream Mach number 0.2. A grid system consisting of $66 \times 151 \times 100$ grid points is used with 37 points in the axial direction and 80 points in the spanwise direction located on the wing. The minimum spacing at the surface is $\Delta z = 0.00001$ and a uniform spacing along the leading edge, $\Delta y = 0.00011$, is specified.

The numerical calculations for this case were found to be unsteady unless a coarse grid is employed. The unsteadiness in the calculations is attributed to a Kelvin-Helmholtz-type instability of the shear layer which emanates from the leading edge of the delta wing and forms the primary vortex. This unsteady flowfield is characterized by the formation and shedding of small-scale shear-layer vortical structures from the leading edge of the delta wing. This behavior is similar to that observed by Gad-el-Hak and Blackwelder in their water tunnel experiments.[1]

A comparison of the average surface pressure at several axial locations along the wing with the experimental data of Hummel[20] is given in Fig. 4. The calculated results compare well with the experimental data showing only a slightly greater expansion in the region below the core of the primary vortex. The overprediction of the pressure at $x = 0.9$ is consistent with the calculations of Thomas[21] and is due in part to the onset of transition near the trailing edge in the experiment. Further details of these computations, including a discussion of the effects of grid resolution, time step, damping, and thin-layer vs full Navier-Stokes equations, may be found in Ref. 10. It should also be noted that computations carried out by

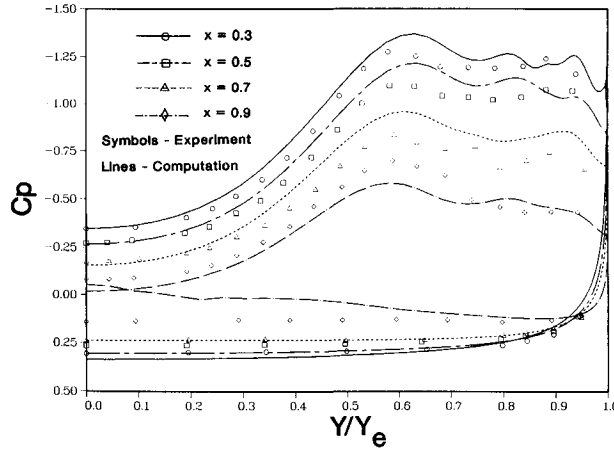

Fig. 4 Comparison of time-averaged surface pressure with experiment[20]: $\alpha = 20.5$ deg, $Re = 900{,}000$.

the present authors for a delta wing using an O-H grid topology have also shown this unsteady shear layer behavior.

An investigation of the effect of time resolution on the unsteady behavior of the high Reynolds number case is carried out. Two values of Δt are considered: 1) $\Delta t = 0.001$ and 2) $\Delta t = 0.00025$. Three subiterations are used for each step at $\Delta t = 0.001$. The pressure is monitored at points traversed by the small scale vortices shed from the leading edge. Results for both time steps at an axial location $x = 0.3$ are given in Fig. 5. This location provided the highest computed frequency and should therefore be the most sensitive to time step resolution. The nondimensional frequency for the smaller time step, $St \approx 24$ ($St = fL/U_\infty$, where L is the root chord length and f the frequency) is higher than the frequency for the larger time step, $St \approx 20$. The basic nature of the flow remains the same, however. A time step of $\Delta t = 0.000125$ is chosen for subsequent calculations. This time step provides adequate temporal resolution, with approximately 300 time steps per cycle at the highest frequency. No subiterations are necessary for this small time step.

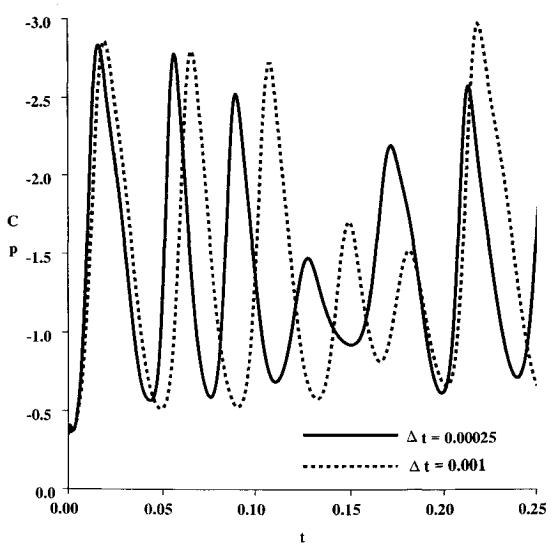

Fig. 5 Comparison of the time histories of pressure for two time steps.

Low Reynolds Number Case

Calculations are also made for a low Reynolds number, $Re = 50{,}000$. This provides several distinct advantages. First, the calculations are in the Reynolds number range of the experiments of Gad-el-Hak[1] and Lowson.[8] Therefore, a better comparison of the computed results with experiment is possible. Secondly, questions involving transition and turbulence that arise at the higher Reynolds number are reduced in importance. Finally, the lower Reynolds numbers results in improved simulations for a given grid size.

The delta wing geometry itself is modeled as a flat plate. This is done to simplify the grid structure in the leading-edge region of the delta wing. It is felt that the underside geometry has no significant effect on the flow physics being investigated.

Calculations for the lower value of Reynolds number are carried out on a $96 \times 151 \times 171$ grid. This grid contains 54 points in the axial direction and 80 points in the spanwise direction on the delta wing with 133 points in the normal direction above the delta wing. The minimum spacing at the wall is $\Delta z = 0.0001$ and the spacing along the leading edge of the delta wing varies from $\Delta y = 0.0005$ at the trailing edge to $\Delta y = 3.165 \times 10^{-5}$ at the apex. The spacing in the axial direction at the apex is $\Delta x = 0.01$ and at the trailing edge, $\Delta x = 0.003$. For the predominant portion of the wing there is a constant axial spacing of $\Delta x = 0.025$. This grid provides enhanced spatial resolution in all three coordinate directions with significant improvements in the resolution of the dominant flow features.

The unsteadiness observed at high values of Reynolds number remains at $Re = 50{,}000$. The unsteady behavior of the flowfield for this case is represented in Figs. 6 and 7. Each figure covers a time period corresponding to approximately one cycle of the unsteady behavior based on the frequency at the axial location, $x = 0.7$.

In Fig. 6, contours of the axial component of vorticity are shown for time $t = 0.4375$ to $t = 0.4875$ on crossplanes located from 0.3 to 0.85. Positive values of vorticity are represented

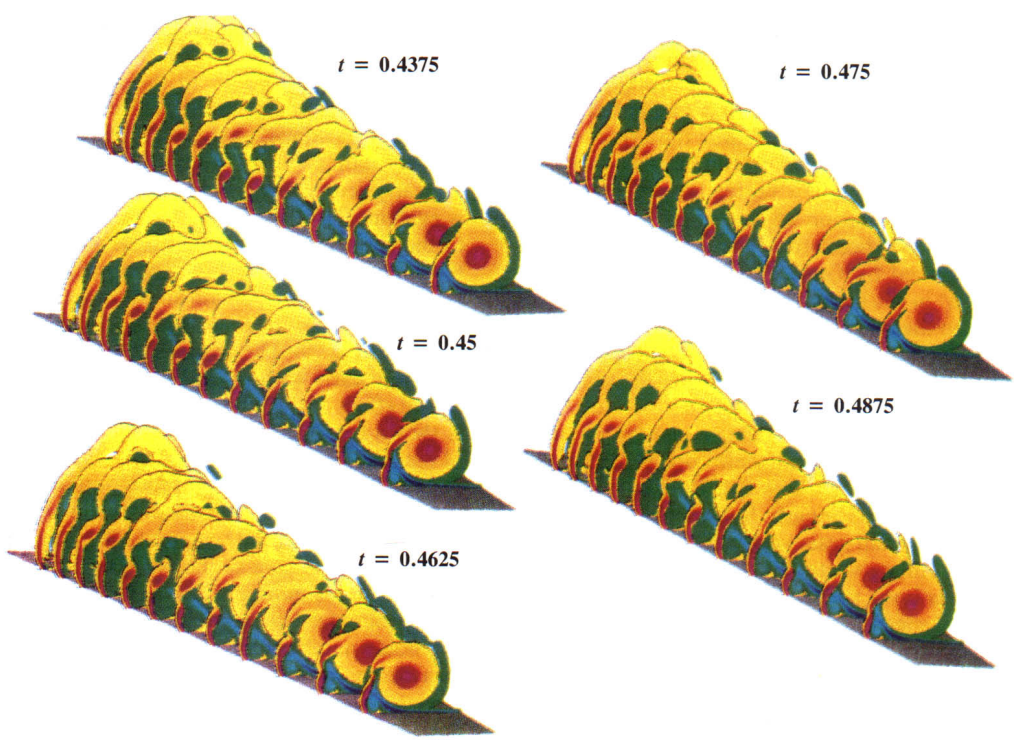

Fig. 6 Three-dimensional unsteady vortex structure $x = 0.3$–0.85, contours of axial component of vorticity.

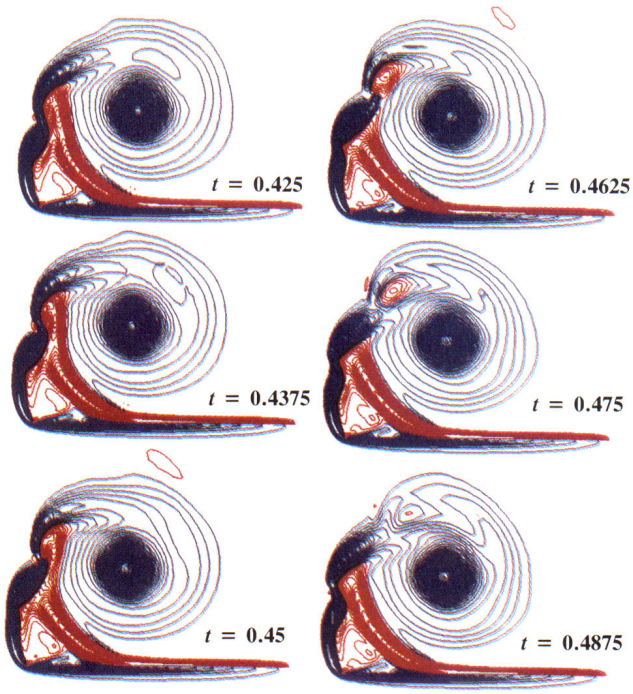

Fig. 7 Unsteady vortex structure, $x = 0.7$, contours of axial component of vorticity: blue > 0, red < 0.

by the colors yellow, red, and magenta, with magenta representing the largest values. Negative values of vorticity are represented by the colors blue, cyan, and green with blue representing the smallest values. The change in sign of vorticity occurs between the green and yellow contours. Clearly visible in the picture are the primary and secondary vortex structures over the delta wing. Also visible are a series of distinct small-scale vortical structures in the shear layer which emanates from the leading edge of the delta wing. These three-dimensional, vortical structures are first evident in the flow at an axial location $x \approx 0.3$. The small-scale vortices consist of a coherent structure that forms first nearer the apex of the delta wing. The structure does not extend initially as a single vortex over the whole length of the leading edge of the delta wing. As the vortex sheds nearer the apex of the delta wing, new parts of the vortical structure are forming further downstream. When the vortex sheds, it is convected around the primary vortex and its strength is dissipated. This process proceeds much more rapidly nearer the apex of the delta wing where the scale of the primary vortex is smaller. As the previous vortex is shed a new vortex is formed to take its place. The temporal evolution of this process is seen in Fig. 6. These small-scale vortices are believed to be the source of the striations observed by Gad-el-Hak (Fig. 1) and also observed by Lowson[8] in his smoke flow visualizations.

Further insight into the unsteady behavior may be obtained by looking at the evolution of the vortical structure for a typical cross plane, $x = 0.7$, Fig. 7. In this figure, contours of the axial component of vorticity are plotted with blue contours being positive and red contours being negative. At time $t = 0.425$, the cycle begins with a small scale vortex (1) starting to form. As time progresses from $t = 0.4375$ to $t = 0.4625$, this vortex grows in size and strength. Subsequently, for $t = 0.4625$ to $t = 0.4875$ the small-scale vortex is shed. The vortex convects around the primary vortex and is dissipated. At time $t = 0.475$ a new shear-layer vortex, vortex 2, starts to form. During this process of shear-layer roll up and vortex shedding an interaction can be observed with the secondary region of vorticity. Vorticity of the opposite sign is shredded from this region and is dissipated along with the small-scale vortex as it is convected along the primary vortex. These figures appear to agree qualitatively with the smoke flow visualizations of Lowson (Fig. 2).

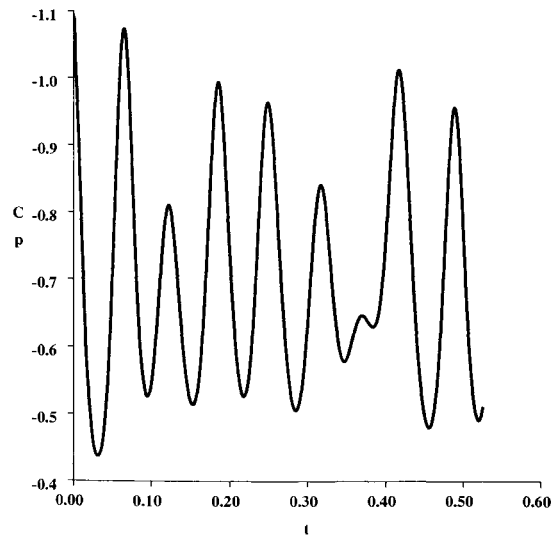

Fig. 8 Typical time history of pressure for the axial location $x = 0.7$.

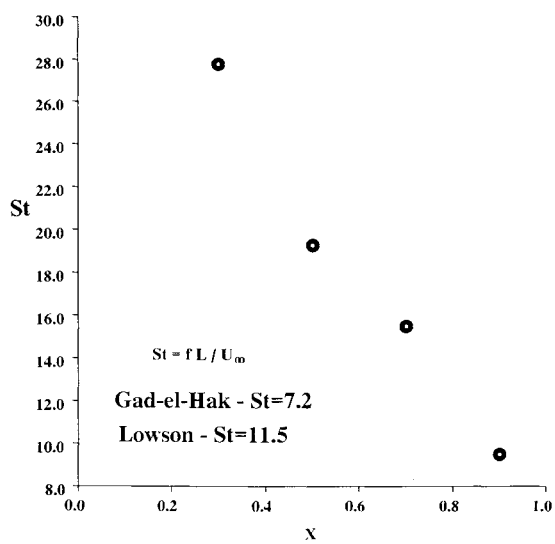

Fig. 9 Shedding frequency as a function of axial location.

The pressure at points in the flowfield where the core of the small-scale, shear-layer vortices pass is monitored at several axial locations. A typical pressure-time history for the axial location $x = 0.7$ is given in Fig. 8. A dominant frequency is clearly seen even though the existence of other harmonics is evident. This dominant frequency is found to correspond to the shedding of the small-scale vortical structures. While the time histories are not sufficiently long to allow for an accurate frequency domain analysis, an average dominant frequency at each location can be found, and the results are shown in Fig. 9. The average frequencies are seen to scale almost linearly with axial distance.

The effect of the unsteady behavior on the surface pressure is shown for axial location $x = 0.7$ (Fig. 10). The shedding of the small-scale vortices contributes to only a small temporal variation of the surface pressure outboard of the core of the primary vortex. This contrasts with the high Reynolds number case[10] where a marked temporal effect on the surface pressure outboard of the core of the primary vortex was seen. For the high Reynolds number the small-scale vortices form and are shed from the leading edge of the delta wing. In the low Reynolds number case the small-scale vortices form further away from the leading edge of the delta wing, therefore, their interaction with the secondary separation region and with the surface flow of the wing is reduced. Time histories of the lift and drag coefficients also show only a slight temporal variation (Fig. 11). The lift coefficient varies by approximately 2.5%

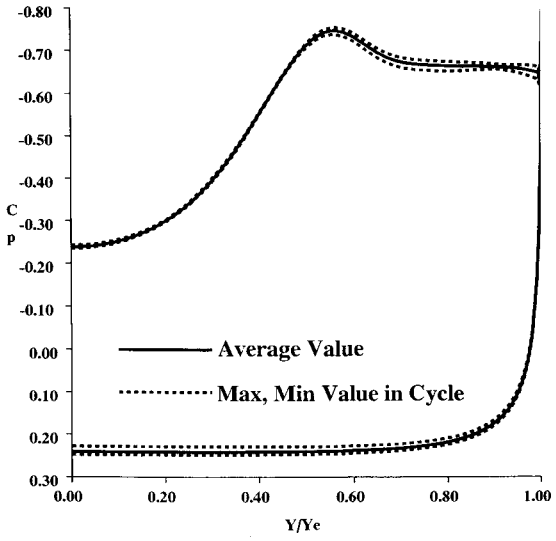

Fig. 10 Comparison of time-averaged surface pressure with the maximum and minimum values for one cycle, $x = 0.7$.

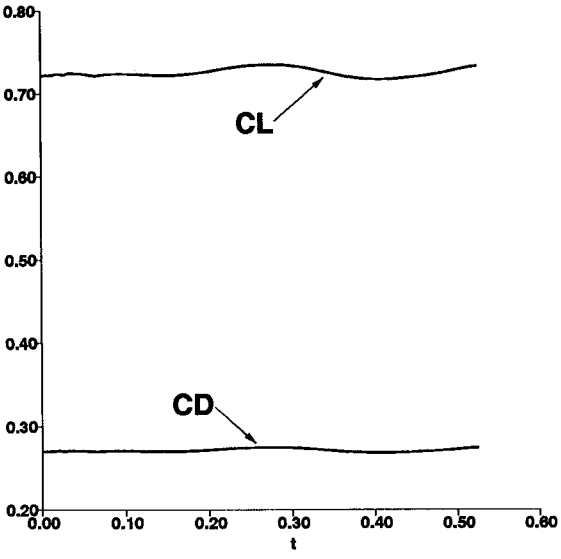

Fig. 11 Time history of lift and drag coefficient.

and the drag coefficient varies by approximately 1.8%. This shows that while the shear layer emanating from the leading edge is unsteady, the primary vortex over the delta wing remains relatively steady.

Discussion

The current calculations show similarities to the flow visualizations of both Gad-el-Hak and Blackwelder[1] and Lowson.[8] Direct comparison of the computations with experiments remains difficult, however. The majority of the results of Lowson, for example, are subject to a 50-Hz wind-tunnel background excitation which is not modeled in the computations. Furthermore, comparisons of smoke and dye flow visualizations with contours of a particular flow variable such as vorticity must be made with care, since the comparison is not exact.[22] With these cautions noted the following observations can be made.

Both Gad-el-Hak and Lowson view the instability as a series of vortices formed and shed from the leading edge of the delta wing at a single frequency. Gad-el-Hak gives an empirical relation for this frequency

$$St = 1625/\sqrt{Re} \tag{2}$$

while Lowson gives the relation

$$St = 2577/\sqrt{Re} \tag{3}$$

This description of the instability is not completely consistent with what is observed in the calculations, however. Here, the small-scale vortices do not form at the leading edge, but further along the vortex sheet. Furthermore, the vortices do not roll up as a single unit along the entire length of the leading edge, but rather form first nearer the apex of the delta wing, and then subsequently further back along the leading edge of the wing. In the case of the experiments of Lowson this difference in character may be attributable to the 50-Hz wind-tunnel excitation of the flowfield forcing the vortices to form at the leading edge.

Rather than a single frequency, an almost linear variation of the frequency of formation of the small-scale vortices is observed, with higher frequencies nearer the apex of the delta wing. For $Re = 50{,}000$, the empirical formula of Gad-el-Hak [Eq. (2)] predicts a frequency, $St = 7.2$, while Lowson's relation [Eq. (3)] predicts a frequency, $St = 11.5$. These values are of the same order as the frequencies computed in the aft portion of the delta wing. Thus, the computed frequencies are consistent with the experimentally measured frequency values.

Further insight into the shear-layer instability is obtained by considering an inviscid, linear stability analysis for a two-dimensional shear layer between coflowing streams. Monkewitz and Huerre[23] considered analytically the case where the mean velocity profile is described by

$$U(y) = 1 + \lambda \tanh(y/2) \tag{4}$$

where $\lambda = (\Delta U/2\bar{U})$ is a measure of the velocity difference across the layer with $\bar{U}$ the average velocity of the two streams and $y = 4y^*/\delta_\omega$, where y^* is the dimensional length and δ_ω is the vorticity thickness. For $\lambda = 1$ the maximum amplified frequency from the linear spatial stability analysis was found to be $\omega = 0.21$ where

$$\omega = (\delta_\omega/4)[(2\pi f)/\bar{U}] \tag{5}$$

This value does not depend strongly on λ.

In an individual crossplane at a given time, the flow which emanates from the leading edge of a delta wing may be viewed as a skewed shear layer. This shear layer may be separated into two components, an axial component and a shear or crossflow component. To a first approximation the stability of the shear component is assumed to be the dominant factor in the stability of the shear layer. If the shedding frequencies at the crossplanes previously considered are nondimensionalized as in Eq. (5), values of ω are obtained in the range $\omega \approx 0.13$–0.32 with the specific value of ω dependent on the shear-layer properties at the location chosen for nondimensionalization. These values of ω are of the same order as the maximum amplified frequency $\omega = 0.21$ found in the spatial stability analysis. Furthermore, a value of $\omega \approx 0.21$ always occurs at the approximate location where the small scale vortices are forming in the shear layer. This simplified analysis indicates that the computed flowfield unsteadiness results from a shear-layer instability. The computed frequencies are consistent with the maximum amplified frequency obtained from a two-dimensional, spatial, linear stability analysis for shear-layer flows.

Pairing of the small-scale vortical structures has been observed in both the experiments of Gad-el-Hak[1] and Lowson.[8] Gad-el-Hak suggests that the primary vortex over the delta wing originates as a series of pairings of the smaller scale vortices shed from the leading edge of the delta wing. However, vortex pairing has not been observed in the experiments of Shi et al.[5] Pairing of the small vortices is also not observed in the computations. The shear layer which emanates from the wing leading edge is expected to be highly susceptible to modification due to external excitation, intentional or unintentional. This excitation of the shear layer could promote the pairing process and is currently not modeled in the computations. In order to obtain a rigorous comparison of com-

putations with experiment, a known forcing frequency might be required in both experiment and computation.

It should also be noted that both experiments[24] and computations[25] for flow over slender bodies of revolution at large incidence exhibit a similar type of shear-layer instability. Small scale, three-dimensional vortices are observed to move along the primary surface of crossflow separation emanating from the body. The high-frequency phenomena observed is distinct from the von Karman-type shedding that occurs at very high incidence for slender bodies of revolution. The experiments[24] and computations[25] compare only qualitatively, but the numerical calculations capture the physical instability.

Finally, computations for the same delta wing and flow properties have been performed by others using several different numerical techniques.[21,26,27] No unsteady flow behavior similar to the instability previously discussed is reported in these references, however. Murman[28] has observed an unsteady flow behavior that results in a lack of convergence of the residual to steady state for Euler calculations over delta wings. The source of the lack of convergence is traced to the existance of unsteady, small-scale vortices in the shear layer from the wing leading edge. Since his computations are not fully time accurate, these observations were only qualitative. Shear-layer, vortical structures have also been observed by Darmofal and Haimes[29] in the computational solutions of Becker[30] for the NASA National Transonic Facility wing. The resolution of these conflicting observations for the computation of delta wing flows requires further study.

Summary

A numerical investigation of the unsteady vortex structure over a 76-deg sweep delta wing at 20.5-deg angle of attack has been carried out. Calculations are performed for a Mach number 0.2 and Reynolds numbers of 50,000 and 900,000. The numerical calculations show that the shear layer which emanates from the leading edge of the delta wing is subject to a Kelvin-Helmholtz-type instability. Small-scale, three-dimensional vortical structures are observed in the shear layer. The small-scale vortices consist of a coherent structure that forms first nearer the apex of the delta wing and subsequently further aft along the leading edge. These vortices are shed and convected around the primary vortex with their strength being dissipated. The frequency of shedding of these small-scale structures is seen to vary nearly linearly with axial location. The observed frequencies are consistent with the maximum amplified frequency found from an inviscid, linear, spatial stability analysis for a two-dimensional, crossflow shear layer. The small-scale vortical structures have been shown to be related to results of several experimental investigations[1,5,6,8] though some differences in the specific character of the computed and experimental structures are noted.

Acknowledgment

The authors wish to thank William Clements, Director of the Computer Center at Eglin Air Force Base, Florida, for providing the computer resources for these calculations.

References

[1]Gad-ed-Hak, M., and Blackwelder, R. F., "The Discrete Vortices from a Delta Wing," *AIAA Journal*, Vol. 23, No. 6, 1985, pp. 961, 962.

[2]Brown, G. L., and Roshko, A., "On Density Effects and Large Structure in Turbulent Mixing Layers," *Journal of Fluid Mechanics*, Vol. 64, July 1974, pp. 775–816.

[3]Winant, C. D., and Browand, F. K., "Vortex Pairing: The Mechanism of Turbulent Mixing-Layer Growth at Moderate Reynolds Number," *Journal of Fluid Mechanics*, Vol. 63, April 1974, pp. 237–255.

[4]Rediniotis, O. K., Telionis, D. P., and Stapountzis, H., "Periodic Vortex Shedding over Delta Wings," AIAA Paper 89-1923, June 1989.

[5]Shi, Z., Wu, J. M., and Vakili, A. D., "An Investigation of Leading-Edge Vortices on Delta Wings with Jet Blowing," AIAA Paper 87-0330, Jan. 1987.

[6]Payne, F. M., Ng, T. T., Nelson, R. C., and Schiff, L. B., "Visualization and Wake Surveys of Vortical Flow over a Delta Wing," *AIAA Journal*, Vol. 26, No. 2, 1988, pp. 137–143.

[7]Payne, F. M., Ng, T. T., Nelson, R. C., and Schiff, L. B., "Visualization and Flow Surveys of the Leading Edge Vortex Structure on Delta Wing Planforms," AIAA Paper 86-0330, Jan. 1986.

[8]Lowson, M. V., "The Three Dimensional Vortex Sheet Structure on Delta Wings," *Fluid Dynamics of Three-Dimensional Turbulent Shear Flows and Transition*, AGARD-CP-438, Çeşme, Turkey, Oct. 1988, pp. 11-1–11-16.

[9]Campbell, J. F., Chambers, J. R., and Rumsey, C. L., "Observation of Airplane Flowfields by Natural Condensation Effects," *Journal of Aircraft*, Vol. 26, No. 7, 1989, pp. 593–604.

[10]Gordnier, R. E., and Visbal, M. R., "Unsteady Navier-Stokes Solutions for a Low Aspect Ratio Delta Wing," AIAA Paper 90-1538, June 1990.

[11]Pulliam, T. H., and Steger, J. L., "Implicit Finite-Difference Simulation of Three-Dimensional Compressible Flows," *AIAA Journal*, Vol. 18, No. 2, 1980, pp. 159–167.

[12]Beam, R. M., and Warming, R. F., "An Implicit Factored Scheme for the Compressible Navier-Stokes Equations," *AIAA Journal*, Vol. 16, No. 4, 1978, pp. 393–402.

[13]Jameson, A., Schmidt, W., and Turkel, E., "Numerical Solutions of the Euler Equations by Finite Volume Methods Using Runge-Kutta Time-Stepping Schemes," AIAA Paper 81-1259, June 1981.

[14]Simpson, L. B., and Whitfield, D. L., "A Flux-Difference Split Algorithm for Unsteady Thin-Layer Navier-Stokes Solutions," AIAA 9th Computational Fluid Dynamics Conf., AIAA Paper 89-1995-CP, Buffalo, NY, June 1989, pp. 634–642.

[15]Visbal, M. R., "Numerical Investigation of Laminar Juncture Flows," AIAA Paper 89-1873, June 1989.

[16]Visbal, M. R., "Structure of Laminar Juncture Flows," *AIAA Journal*, Vol. 29, No. 8, 1991, pp. 1273–1282.

[17]Webster, W. P., and Shang, J. S., "Thin-Layer Full Navier-Stokes Simulations over a Supersonic Delta Wing," *AIAA Journal*, Vol. 29, No. 9, 1991, pp. 1363–1369.

[18]Stanek, M. J., and Visbal, M. R., "Investigation of Vortex Development on a Pitching Slender Body of Revolution," AIAA Paper 91-3273, Sept. 1991.

[19]Whitfield, D. L., "Three-Dimensional Unsteady Euler Equation Solutions Using a Flux Vector Splitting," Short Course on Numerical Grid Generation at Mississippi State Univ., Mississippi State, MS, June 1984.

[20]Hummel, D., "On the Vortex Formation over a Slender Wing at Large Angles of Incidence," *High Angle of Attack Aerodynamics*, AGARD-CP-247, Sandefjord, Norway, Oct. 1978, pp. 15-1–15-17.

[21]Thomas, J. L., Krist, S. L., and Anderson, W. K., "Navier-Stokes Computations of Vortical Flows over Low Aspect Ratio Wings," *AIAA Journal*, Vol. 28, No. 2, 1990, pp. 205–212.

[22]Gursul, I., Lusseyran, D., and Rockwell, D., "On Interpretation of Flow Visualization of Unsteady Shear Flows," *Experiments in Fluids*, Vol. 9, No. 5, 1990, pp. 257–266.

[23]Monkewitz, P. A., and Huerre, P., "Influence of the Velocity Ratio on the Spatial Instability of Mixing Layers," *Physics of Fluids*, Vol. 25, No. 7, 1982, pp. 1137–1143.

[24]Degani, D., and Zilliac, G. G., "Experimental Study of Nonsteady Asymmetric Flow Around an Ogive-Cylinder at Incidence," *AIAA Journal*, Vol. 28, No. 4, 1990, pp. 642–649.

[25]Schiff, L. B., Degani, D., and Gavali, S., "Numerical Simulation of Vortex Unsteadiness on Slender Bodies of Revolution at Large Incidence," AIAA Paper 89-0195, Jan. 1989.

[26]Kandil, O. A., and Chuang, H. A., "Unsteady Delta-Wing Flow Computation Using an Implicit Factored Euler Scheme," *AIAA Journal*, Vol. 28, No. 9, 1990, pp. 1589–1595.

[27]Ekaterinaris, J. A., and Schiff, L. B., "Vortical Flows over Delta Wings and Numerical Prediction of Vortex Breakdown," AIAA Paper 90-0102, Jan. 1990.

[28]Murman, E. M., and Rizzi, A., "Applications of Euler Equations to Sharp Edge Delta Wings with Leading Edge Vortices," *Applications of Computational Fluid Dynamics in Aeronautics*, AGARD-CP-412, Aix-en-Provence, France, April 1986, pp. 15-1–15-13.

[29]Darmofal, D., and Haimes, R., "Visual Feature Identification for 3-D Data Sets," AIAA 10th Computational Fluid Dynamics Conf., AIAA Paper 91-1583-CP, Honolulu, HI, June 1991, pp. 638–647.

[30]Becker, T., "Hybrid 3-D Euler/Navier-Stokes Calculations of Transonic Vortex Flows over the NTF Delta Wing," M.S. Thesis, Massachusetts Inst. of Technology, Dept. of Aeronautics and Astronautics, Cambridge, MA, Aug. 1989.